



Contents lists available at ScienceDirect

Applied Soft Computing

journal homepage: www.elsevier.com/locate/asoc

A study on fuzzy clustering for magnetic resonance brain image segmentation using soft computing approaches

Sanjay Agrawal^a, Rutuparna Panda^{a,*}, Lingraj Dora^b^a Department of Electronics & Telecommunication Engineering, VSS University of Technology, Burla 768018, India^b Department of Electrical & Electronics Engineering, VSS University of Technology, Burla 768018, India

ARTICLE INFO

Article history:

Received 21 February 2013

Received in revised form 2 July 2014

Accepted 6 August 2014

Available online xxx

Keywords:

Fuzzy C-means (FCM) clustering

K-means clustering

Genetic algorithm (GA)

Particle swarm optimization (PSO)

Bacteria foraging optimization (BFO)

ABSTRACT

This paper presents a novel idea of intracranial segmentation of magnetic resonance (MR) brain image using pixel intensity values by optimum boundary point detection (OBPD) method. The newly proposed (OBPD) method consists of three steps. Firstly, the brain only portion is extracted from the whole MR brain image. The brain only portion mainly contains three regions – grey matter (GM), white matter (WM) and cerebrospinal fluid (CSF). We need two boundary points to divide the brain pixels into three regions on the basis of their intensity. Secondly, the optimum boundary points are obtained using the newly proposed hybrid GA–BFO algorithm to compute final cluster centres of FCM method. For a comparison, other soft computing techniques GA, PSO and BFO are also used. Finally, FCM algorithm is executed only once to obtain the membership matrix. The brain image is then segmented using this final membership matrix. The key to our success is that we have proposed a technique where the final cluster centres for FCM are obtained using OBPD method. In addition, reformulated objective function for optimization is used. Initial values of boundary points are constrained to be in a range determined from the brain dataset. The boundary points violating imposed constraints are repaired. This method is validated by using simulated T1-weighted MR brain images from IBSR database with manual segmentation results. Further, we have used MR brain images from the Brainweb database with additional noise levels to validate the robustness of our proposed method. It is observed that our proposed method significantly improves segmentation results as compared to other methods.

© 2014 Published by Elsevier B.V.

Introduction

Image segmentation has been a very critical and important stage in any image processing application. It deals with dividing the pixels in an image into groups or regions having similar features or characteristics for effective object identification. The segmentation of magnetic resonance (MR) brain image has got significant focus in the field of biomedical image processing. Segmentation of MR brain image has got wide application in the field of bio-medical analysis, such as identification of tumours, classification of tissues and blood cells, multi modal registration [1] etc. There are various segmentation techniques proposed for MR brain image like thresholding [2], edge based detection [3] and region growing [4].

Thresholding techniques are effectively used when the histograms of the objects and background are clearly identifiable. But for brain image, these techniques give the inaccurate segmentation result as distribution of pixels in brain image is very complex. Edge based methods rely heavily on detection of boundaries in the image. It is observed in the brain image that grey level distribution of pixels of grey matter (GM), white matter (WM) and cerebrospinal fluid (CSF) result in incorrect detec-

tion of boundary. Region growing techniques use the homogeneity and connectivity criteria for segmentation. It is not effectively used for brain image segmentation as the brain image does not contain well defined regions. The above methods are found effective for relatively simple images.

So one of the efficient techniques used for complex brain image segmentation is clustering. It classifies the pixels into larger groups depending on certain criteria. Again, several types of clustering methods have been discussed in literature like Expectation–maximization [5], hard C-means, K-means and fuzzy clustering techniques [6]. Among fuzzy clustering techniques, fuzzy C-means (FCM) is the most widely used technique [7,8]. It aims at minimizing an objective function according to some criteria. It permits one data point to belong to more than one cluster defined by a membership matrix. But the random selection of centroids makes the technique fall into local optimum. To overcome this problem, soft computing approaches like genetic algorithm (GA) [9–11], Particle swarm optimization (PSO) [12], ant colony optimization (ACO) [13] etc. have been applied to improve FCM. Castillo et al. [14] presented optimization of the FCM algorithm by using evolutionary methods. They used GA and PSO only. They used it to find the optimal number of clusters and the weight exponent for different types of synthetic datasets. They emphasized on cluster validation. Hruschka et al. [15] presented a survey of evolutionary algorithms for clustering. They emphasized on partition algorithms that focused on hard clustering of data. The survey did not use any particular evolutionary method, but focused on advanced topics like multi-objective and ensemble based evolutionary clustering. Then a taxonomy that highlights on some very important aspects of evolutionary clustering was presented at the end.

* Corresponding author. Tel.: +91 6632431857; fax: +91 6632430204.

E-mail addresses: lingraj02uce157ster@gmail.com, agrawals.72@yahoo.com (S. Agrawal), r.panda@yahoo.co.in (R. Panda), lingraj02uce157ster@gmail.com (L. Dora).

Mukhopadhyay and Maulik [16] proposed a multiobjective real coded genetic fuzzy clustering scheme for the segmentation of multispectral MR images of the human brain. Their technique is able to determine the number of clusters along with clustering results. They emphasized on including the spatial information for improved segmentation result.

All the above mentioned approaches emphasize on selecting a random initial cluster centre for FCM. Then evolutionary computing techniques are used to obtain optimum cluster centroids. FCM is then iteratively applied to obtain a final membership matrix for segmentation. However, in this paper, a new strategy for intracranial (also coined as brain extraction) segmentation of MR brain image using hybridized fuzzy C-means clustering technique is proposed. Instead of randomly selecting centroids of clusters and optimizing them, we have used OBPD method. We first determine the number of boundary points from the dataset to divide the region into required number of clusters. These boundary points are optimized using a new hybrid GA–BFO technique. Other soft computing approaches GA, PSO and BFO are also used for a comparison. We have also used a classical method coined as K-means clustering for a comparison. Final centroids of the clusters are then computed. These final centroids are used to obtain the fuzzy membership matrix by executing FCM once only. To the best of our knowledge, hybrid GA–BFO has not been used so far for MR brain image segmentation. This has motivated us to use the proposed technique.

It has already been reported in the literature that a brain image mainly consists of three regions: grey matter (GM), white matter (WM) and cerebrospinal fluid (CSF) [9,17]. The grey level distribution is used to identify these three regions. For accurate identification, ideal clustering is needed.

Two optimum boundary points are obtained from the grey level distribution to divide the brain image into three regions or clusters. Initial values of the boundary points are constrained to be in a range determined from the brain dataset. The proposed study aims at optimizing these boundary points by using hybrid GA–BFO technique to select final cluster centres for FCM algorithm. The objective function used is reformulated in terms of cluster centres only. Using the final cluster centres, the proposed hybrid FCM algorithm is executed only once to obtain the fuzzy membership matrix. Segmentation is then done using this fuzzy membership matrix. Several standard brain images (simulated T1-weighted) from the IBSR database with manual segmentation results are considered in the experiment. The results obtained are compared using various performance parameters. The segmentation performance parameters are also calculated for different noise levels. For the experiment, we consider brain images from Brainweb database with additional noise levels: 1%, 3%, 5%, 7% and 9%. Results are presented in ‘Results and discussions’ section to validate the robustness of our proposed method.

The rest of the paper is organized as follows. ‘FCM and soft computing methods’ section presents a brief introduction about FCM technique and soft computing approaches i.e. GA, PSO, BFO and GA–BFO. ‘Proposed methodology’ section explains the proposed methodology. ‘Results and discussions’ section presents the results and discussions. The last section is the conclusion.

FCM and soft computing methods

Fuzzy C-means clustering (FCM) algorithm

Fuzzy clustering allows objects to belong to more than one cluster by specifying a membership matrix with different degree for each cluster. It is a local optimum search technique. In this algorithm, a set of n objects $x = \{x_1, x_2, \dots, x_n\}$ each having d dimensions are divided into c number of clusters of similar features. The features could be the position or intensity of a pixel in an image. The fuzzy clusters of objects are characterized by a fuzzy membership matrix with n rows and c columns. The set of all constrained fuzzy matrices of size $n \times c$ is defined as [8]:

$$M_f = \left\{ \mu \in \mathbb{R}^{n \times c} \mid \sum_{j=1}^c \mu_{ij} = 1, \quad 0 < \sum_{i=1}^n \mu_{ij} < n, \quad \mu_{ij} \in [0, 1] \right\} \quad (1)$$

for $1 \leq i \leq n; 1 \leq j \leq c$.

The condition used to define good clusters for FCM is to minimize the FCM function [8]:

$$J_m(\mu, z) = \sum_{j=1}^c \sum_{i=1}^n (\mu_{ij})^m d_{ij}^2(z_j, x_i), \quad (2)$$

where μ is the fuzzy membership matrix, $1 \leq m \leq \infty$ is a scalar weighting exponent which controls the fuzziness. The larger is its

Table 1
Parameter setting for the different methods.

The parameter setting for FCM is:
<ul style="list-style-type: none"> • Scalar weighting exponent $m = 2$, • Number of iterations = 20, • Number of clusters = 3
The parameter setting for GA–FCM is:
<ul style="list-style-type: none"> • Number of iterations = 20, • Population number = 20 • Crossover probability = 0.8, • Mutation probability = 0.05 • Selection function is the Roulette wheel selection
The parameter setting for PSO–FCM is:
<ul style="list-style-type: none"> • Number of iterations = 20, • Number of particles = 20, • Acceleration coefficients $C_1 = C_2 = 2$ • Weight factor $w = 0.9$
The parameter setting for GA–BFO–FCM (proposed method) is:
<ul style="list-style-type: none"> • Number of bacteria = 20, • Number of chemotactic steps = 4, • Swimming length = 10, • Number of reproduction steps = 4, • Number of elimination and dispersal event = 2 • Probability of elimination and dispersal = 0.02 • Probability of crossover = 0.7 • Mutation probability = 0.01

value, fuzzier is the partition. An analysis on the weighting exponent is found in Ref. [18]. When the value of m is close to 1, FCM approaches hard c-means algorithm. When m approaches infinity, the mass centre of the data set is the only solution of FCM [18]. Here the value of m is set to 2. It is observed that this value of m is suitable for most MR brain images, as it yield best results [19]. Note that $z = [z_1, z_2, \dots, z_c]$ is a matrix of cluster centres, and $d_{ij}(z_j, x_i)$ is a measure of Euclidean distance from x_i to j th cluster centre z_j . The algorithm used in this paper is presented below:

Algorithm. Step 1: Generate brain portion only data set $x = \{x_1, x_2, \dots, x_n\}$ of MR brain images.

Step 2: Set various parameters (like the scalar weighting exponent m) and the termination condition i.e. the maximum number of iterations.

Step 3: Select the number of clusters c .

Step 4: Get initial set of random cluster centres $z = [z_1, z_2, \dots, z_c]$.

Step 5: Calculate Euclidean distance $d_{ij}(z_j, x_i)$ for $i = 1, 2, \dots, n; j = 1, 2, \dots, c$.

Step 6: Calculate membership matrix μ_{ij} using Eq. (3) as:

$$\mu_{ij} = \frac{1}{\sum_{k=1}^c (d_{ij}/d_{ik})^{2/m-1}} \quad \text{for } i = 1, 2, \dots, n; \quad j = 1, 2, \dots, c \quad (3)$$

Step 7: Update the cluster centres z_j using the membership matrix μ_{ij} by using Eq. (4) as:

$$z_j = \frac{\sum_{i=1}^n \mu_{ij}^m x_i}{\sum_{i=1}^n \mu_{ij}^m} \quad (4)$$

Step 8: If the termination condition is not met, go to step 5.

In this paper, the parameters for FCM are set as given in Table 1. The algorithm is implemented using MATLAB. The pixels of the brain only portion are clustered using the cluster centres z_j obtained after the termination condition is met. Segmentation of the brain image is done using the final membership matrix μ_{ij} .

Soft computing methods

It may be reiterated the fact that the brain portion mainly contains three regions WM, GM and CSF. The pixels in these regions

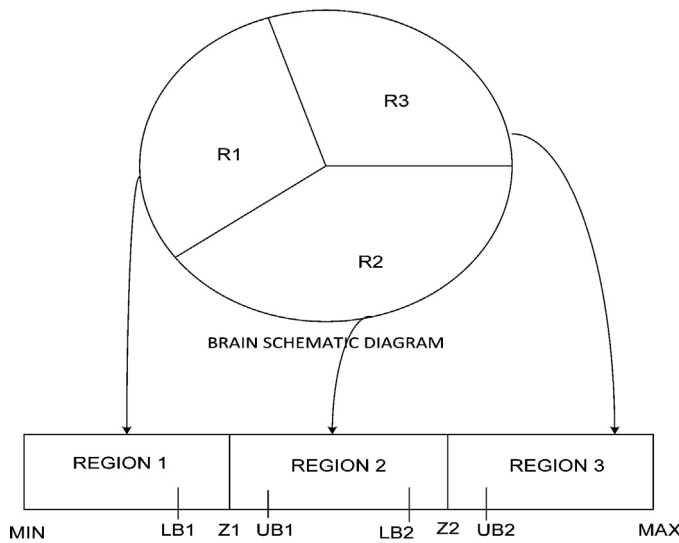


Fig. 1. Pixel values of brain only portion.

have similar intensity values. So we need to group them according to their values. For this reason the grey values of the pixels in the brain image are taken as the basis for clustering. It is worthy to mention here that we need only two optimum boundary points to divide the pixels in the brain image into three regions. In this work, we use hybrid GA–BFO technique to obtain the optimal boundary points. The initial values of the boundary points are constrained to be in a range which is determined from the brain data set. These constraints are even checked inside the soft computing algorithms while updating their values. Here, we also suggest a repairing mechanism for constraint violation. In this connection, we introduce a new constrained optimization problem. When updated boundary points cross their lower or upper bounds, they are repaired by taking the old boundary values or replacing them with a newly generated random value within the bound. This step enhances the accuracy of a clustering because if the boundary points cross the bounds, then the pixels may be clustered in a wrong region. The idea is presented in Fig. 1.

Let two boundary points be represented as $[z_1, z_2]$. The constraints are introduced such that $LB_1 < z_1 < UB_1$ and $LB_2 < z_2 < UB_2$. Here LB represents lower bound and UB represents upper bound. A value of z_1 or z_2 is checked for constraint violation and the repair is done as:

$$z_1 = \begin{cases} z_1 & \text{if } LB_1 < z_1 < UB_1 \\ LB_1 + rand \cdot (UB_1 - LB_1) & \text{otherwise} \end{cases} \quad (5)$$

$$z_2 = \begin{cases} z_2 & \text{if } LB_2 < z_2 < UB_2 \\ LB_2 + rand \cdot (UB_2 - LB_2) & \text{otherwise} \end{cases} \quad (6)$$

where *rand* denotes random number. This helps in reducing the percentage of misclassification and increasing the accuracy in segmentation.

The objective function for our study is reformulated as [20].

$$F_m(z) = \sum_{j=1}^n \left(\sum_{i=1}^{\eta} d_{ij} (1/(1-m)) \right)^{(1-m)} \quad (7)$$

where d_{ij} is the Euclidean distance from x_j to i th cluster centre. Here x_j is the feature vector of the brain image matrix x having a dimension of $p \times n$. Note that n represents the number of feature vectors (pixel numbers in the brain image) and p represents the dimension of each feature vector. The fitness function (7) is

different from Eq. (2) in the sense that its dependence on membership matrix is removed.

GA–FCM algorithm

The genetic algorithm (GA) is a global search technique that imitates the theory of biological evolution. It operates on the basic principle of survival of the fittest [21]. A set of chromosomes (or parents) represents a set of initial solutions called population. A new population (offspring) is evolved by taking solutions from the old population. The new population is selected according to their fitness values. The older population is discarded and a new population is evolved until some stopping criterion is reached. The entire process of GA–FCM is summarized as follows:

1. A random population of N chromosomes (parents) is generated depending on the problem definition.
2. The fitness value of each chromosome is calculated according to a predefined objective function.
3. A new population (offspring) is evolved by following the steps given below until it is complete, i.e. the number of chromosomes is again same as in the beginning.
 - a. *Selection*: two parent chromosomes are selected from the initial population depending on their fitness value (higher fitness value is usually preferred). Many selection techniques are described in the literature [17], the roulette wheel approach is usually adopted.
 - b. *Crossover*: the parent chromosomes crossover to generate a new chromosome (offspring) using a pre-defined crossover probability.
 - c. *Mutation*: at each position, some chromosomes are altered at random with a pre-defined mutation probability to facilitate GA with some local optimum searching ability.

The new offspring is then placed in the new population. The whole process from step 2 is repeated until the stopping criterion is reached. The algorithm implemented in this paper is as follows:

As stated before, segmentation of the brain image is achieved by using the pixel values. The minimum value MIN and maximum value MAX of the pixels are taken from the extracted brain only portion. Because the brain image contains three regions, two boundary points Z_1 and Z_2 are needed as shown in Fig. 1. The values of Z_1 and Z_2 are constrained to be in the range as defined by LB and UB, which represent the lower and upper bound for the boundary points respectively. These bounds are checked for constraint violation and repair using Eqs. (5) and (6). The fitness function as defined in Eq. (7) is used for optimization. Since only the cluster centres z_j are used in GA based clustering, fitness function (7) is used. Here we have implemented GA using the GA solver in the OPTIM toolbox of MATLAB. The parameter setting for GA–FCM is given in Table 1. The number of boundary points is represented by the dimension of the search space. A minimum value of F_m in Eq. (7) results in optimum boundary points. After getting the boundary points Z_1 and Z_2 , the brain image is divided into three clusters or regions. Then the final three cluster centroids are calculated. Using these final cluster centroids, FCM algorithm is executed once only, to get the fuzzy membership matrix as defined in Eq. (3). Segmentation is then achieved by using this fuzzy membership matrix.

PSO–FCM algorithm

Eberhart and Kennedy [22] proposed a population based evolutionary optimization technique called particle swarm optimization (PSO). It is based on the social behaviour of birds or fish while searching food. An individual is identified as a particle in PSO with a predefined location. The search space is identified by a dimension D which represents the search space of the problem or function. For each particle, an objective function is evaluated at its

current location. The particle, then moves in the search space with a dynamically adjusted velocity according to its own experience and its neighbour's experience thereby moving to a new location. The process is continued until all the particles in the population have moved to their new locations. Finally, all the particles will move to a location where an optimum value of the objective function is achieved.

Each particle in a population has a current location, a previous best location and a velocity. But the population has an overall best location. The current location is assumed a problem solution. The previous best location (i.e. location giving the best objective function value) is identified as a variable $pbest$. The overall best location (i.e. location giving the best objective function value by any particle in the population) is identified as a variable $gbest$. The current location is continuously updated and new solutions are obtained by evaluating the objective function. The current locations are modified by adding a dynamically adjusted velocity as given:

$$v_{t+1} = w \times v_t + c_1 \times rand \times (pbest - x_t) + c_2 \times rand \times (gbest - x_t) \quad (8)$$

$$x_{t+1} = x_t + v_{t+1} \quad (9)$$

where c_1 and c_2 represent acceleration constant, $rand$ is the random function, w is the inertia weight, v_{t+1} is the updated velocity, x_{t+1} is the updated current location of a particle.

It is compared with $pbest$ and then $pbest$ is updated. From the $pbest$ values, $gbest$ value is evaluated. Thus, in PSO at each step, a particle moves towards its $pbest$ and $gbest$ locations by updating its velocity.

The algorithm of PSO–FCM implemented for fuzzy clustering is presented below:

Algorithm. *Step 1:* Set the parameters of PSO, scalar weighting exponent m and stopping criteria as maximum number of iterations.

Step 2: Generate a swarm with P particles. Initialize the position x of particles which represent the number of boundary points. Check for constraint violation and repair using Eqs. (5) and (6).

Step 3: Initialize velocity, $pbest$ and $gbest$ for the particles.

Step 4: Calculate the fitness value for each particle using Eq. (7).

Step 5: Calculate $pbest$ value for each particle and $gbest$ value for the swarm.

Step 6: Update the velocity of each particle using Eq. (8).

Step 7: Update the position of each particle using Eq. (9) subject to the constraints defined in Eqs. (5) and (6).

Step 8: If the termination condition is not met, go to step 4.

In this paper, we have implemented the algorithm using MATLAB. The stopping criterion is the maximum number of iterations and is taken as 20. The parameter setting is given in Table 1. A minimum value of the fitness function in Eq. (7) gives us the final boundary points.

Hybrid GA–BFO–FCM algorithm

Passino [23] proposed a nature inspired optimization algorithm based on the foraging technique of *Escherichia coli* bacteria. The bacteria searches for nutrients such that the energy obtained per unit time spent in searching is optimized or maximized. The movement of bacteria in this foraging technique has been discussed in four important steps [24].

a) *Chemotaxis:* this step explains the movement of bacteria through swimming and tumbling. A bacterium may swim or tumble depending on the food concentration and environment condition. If the condition is favourable then it continues to swim for a pre-defined number of steps, otherwise it tumbles. These

two movement processes continue for the entire lifetime of the bacterium.

b) *Swarming:* during the process of foraging and maximizing the energy obtained per unit time spent, the bacterium which has searched the optimum path should attract the other bacteria by sending some signal. This will help the bacteria in concentrating themselves as a swarm and move towards the optimum location.

c) *Reproduction:* this step shows the survival of the fittest character. The energy obtained per unit time spent for each bacterium is sorted and the bacterium having the highest values are declared not healthy and hence die. The remaining bacteria are considered healthy and fit to reproduce (split into two) and are kept in the same location making the bacteria count same. Here we have used the crossover and mutation operation of GA to improve the result.

d) *Elimination and dispersal:* this step eliminates some bacteria due to some disturbances in the environment like increase in heat killing the bacteria. This may also disperse some bacteria to a new location by change in condition like flow of water.

The algorithm for the above technique is presented as follows:

Step 1: Set the parameters of GA–BFO and scalar weighting exponent m .

Step 2: Initialize the position P of each bacterium which represents the boundary points. Check for constraint violation and repair using Eqs. (5) and (6).

Step 3: Increment the elimination–dispersal loop $l = l + 1$.

Step 4: Increment the reproduction loop $k = k + 1$.

Step 5: Increment the chemotaxis loop $j = j + 1$.

- a. For each bacterium i a chemotactic step is taken as,
- b. Calculate nutrient function $J(i, j, k, l)$ for each bacterium.
- c. Save $J_{last} = J(i, j, k, l)$ as better value may be obtained in the future.
- d. Tumble: generate a random vector $rand$ with each element in $[-1, 1]$.
- e. Move: Let

$$P(i, j + 1, k, l) = P(i, j, k, l) + C(i) \cdot \frac{rand(i)}{\sqrt{rand^T(i) \cdot rand(i)}} \quad (10)$$

This operation results in a step of size $C(i)$ in the direction of tumble for bacterium i .

- f. Calculate $J(i, j + 1, k, l)$
- g. Swim:

- i. Initialize the counter for swim length = 0.
- ii. While counter less than the swimming length.

- Increment the counter.
- If $J(i, j + 1, k, l) < J_{last}$, let $J_{last} = J(i, j + 1, k, l)$. Update the position P using the step size $C(i)$ as

$$P(i, j + 1, k, l) = P(i, j + 1, k, l) + C(i) \cdot \frac{rand(i)}{\sqrt{rand^T(i) \cdot rand(i)}} \quad (11)$$

and use this P to calculate the new $J(i, j + 1, k, l)$ as in step (f).

- Continue the above steps till counter equal the swimming length.

h. go to the next bacterium ($i + 1$) i.e. step 5b till all the bacteria are exhausted.

Step 6: If $j <$ number of chemotactic steps, continue the chemotaxis loop and go to step 5.

Step 7: Reproduction:

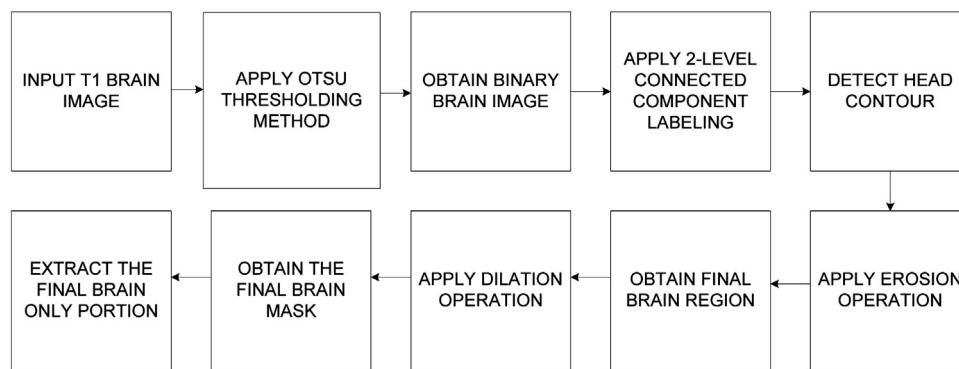


Fig. 2. Block diagram of process for brain only portion extraction.

a. for given k , l and for each bacterium i let

$$J_{\text{health}}^i = \sum_{j=1}^{N_c+1} J(i, j, k, l)$$

be the health of the bacteria i . Then sort the bacteria and the chemotactic parameter in ascending order of J_{health} .

b. The bacteria with highest J_{health} values die and remaining bacteria with best values are treated as parent bacteria for the next generation. However, in GA–BFO the idea of crossover mechanism from GA is used to search nearby locations by positioning 50% of the bacteria randomly at different locations. We get some more missing nutrients through the application of this process. In fact, GA–BFO supplements crossover feature of GA to generate better fitness function values.

c. Now two sets of parent bacteria are chosen and they crossover with a pre-defined crossover probability to get the offspring bacteria.

d. Then the parent bacteria and the newly generated offspring bacteria are appended to form the original number of bacteria for the next generation.

e. A mutation of 1% is carried out to improvise results.

Step 8: If $k <$ number of reproduction loop, continue the reproduction loop and go to step 4.

Step 9: Elimination – dispersal:

For a given probability of elimination and dispersal p_{ed} , eliminate or disperse each bacterium while keeping the population of bacteria constant.

Step 10: If $l <$ elimination–dispersal loop, continue the elimination–dispersal loop and go to step 3. Otherwise end the process.

In this paper, we have implemented GA–BFO algorithm with MATLAB. The parameter setting is given in Table 1. A minimum value of the fitness function in Eq. (7) gives the final boundary points. The brain image is then segmented using the fuzzy membership matrix as explained above.

Proposed methodology

This section explains the proposed methodology of optimizing the fuzzy clustering algorithm for intracranial MR brain image segmentation by using optimum boundary point detection (OBPD). Fuzzy clustering techniques reported earlier fall into local minima because of the random selection of centroids and results in inaccurate segmentation results. Here, an attempt is made to overcome this problem using evolutionary computation (EC)

approaches. The boundary points are optimized using various soft computing approaches. Final centroids are obtained followed by clustering using the fuzzy membership matrix as in the FCM. The MR brain image is then segmented using the cluster information. T1-weighted MR coronal slice taken from MRI data set of 20 normal subjects with manual segmentation results (ground truth) available in IBSR database are considered here to experiment [25].

The MR brain image contains non-brain regions like skull, scalp, fat etc. [26]. So it is first necessary to remove the non-brain portion and extract the brain only portion from the MR image for segmentation. The extracted brain only portion mainly consists of white matter (WM), grey matter (GM) and cerebrospinal fluid (CSF). The proposed study aims at identifying these regions of the brain as accurately as possible. The grey level distribution is used to distinguish the brain portion from the background. The brain region and the non-brain region are distinguished by using region features. Then the brain only region is extracted for clustering and segmentation. The process of extracting the brain only portion is presented as follows:

1. A rough brain image portion is extracted from the MR brain image by using the features of the brain. Usually the brain portion is brighter than the skull and thus, it is preserved in the slice.
2. The rough brain image is converted to binary image by using Otsu's thresholding method [26] which chooses the optimum threshold by maximizing between class variance. This removes objects from the background, if any. The binary image now contains a uniform background, scalp, skull and CSF and brain.
3. The scalp is then separated from the background to produce a head mask by two-level connected component labelling and detecting the contour of the head.
4. The inner dark region representing skull and CSF is then identified by using three stages labelling.
5. The weakly connected region in the rough brain portion is then separated by a morphological operation (erosion) by a disc structuring element having a size depending upon the brain image slice. This step is very crucial. If the erosion is not done accurately, then it may end up removing some vital portion of the brain. This may result in an inaccurate detection of diseased portion of the brain.
6. The final brain region is identified by using the largest connected component from the components of the eroded image.
7. The final brain mask is generated by performing dilation on the identified brain region using the same structuring element. This process helps in recovering the lost pixels due to thresholding and erosion.
8. The brain only portion is extracted by multiplying the original image with the final brain mask.

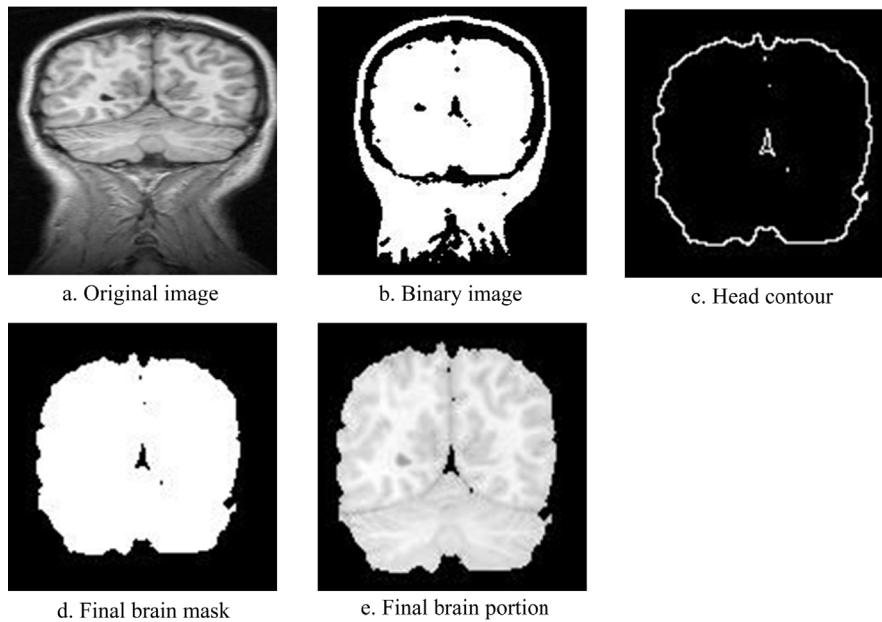


Fig. 3. Brain only image extraction process from MR image.

The block diagram for methodology of extraction of brain only portion is presented in Fig. 2.

T1-weighted MR coronal slice (slice no. 15 of Image 5.8) taken from MRI data set of 20 normal subjects is presented to display the process of extraction of brain only portion in Fig. 3.

After getting the final brain portion from above steps, segmentation is done by using OBPD method.

In this paper, the fitness function (7) does not consider any spatial dependence among the brain image matrix and each image pixel is considered as an individual point. The membership matrix as in Eq. (3) is determined by a measure of similarity between the pixel intensity and cluster centroids. The membership value is higher when the intensity values are closer to the cluster centroids.

In our problem, the feature vectors x_j represent the pixel intensity, its dimension $p = 1$. Here z_i is the i th cluster centre, η represents the number of clusters and m is the scalar weighting constant and is taken as 2. The optimized boundary points computed from Eq. (7) are used to find the final cluster centres in the three regions. Using these final cluster centres, GA–BFO–FCM (proposed method) is executed only once to obtain the fuzzy membership matrix of size $n \times c$. Each term of the fuzzy membership matrix represents the extent of association of j th object with i th cluster centre. The objects nearest to the centroids of their cluster are assigned a high membership value and objects far from these centroids are assigned low membership value. So the pixels in the brain are segmented into three regions according to their membership value. The block diagram for the process of segmentation of brain image is presented in Fig. 4.

The flow chart of the proposed method is presented in Fig. 5.

Results and discussions

Simulated T1-weighted MR coronal slice taken from MRI brain data sets from 20 normal subjects available in IBSR database with the manual segmentation result are used to experiment. The MR images are acquired by 1.5 T General Electric Signa MR System (Milwaukee, WI), with the following parameters: TR = 50 ms, TE = 9 ms, flip angle = 50°, field of view = 24 cm, slice thickness = contiguous 3.0 mm, matrix = 256 × 256.

The images are segmented using K-Means, FCM, GA–FCM, PSO–FCM, BFO–FCM and our proposed technique. It is important to

note that no readily available data for parameters is used for comparison; we have implemented all techniques and generated data for this work. In all the techniques, the fitness function defined in Eq. (7) is used. The scalar weighting exponent m for all the methods used is taken as 2. Results are displayed in the form of tables and figures.

Results are compared using segmentation evaluation indices like Jaccard similarity index, Dice coefficient, false positive rate and false negative rate [27,30]. The Jaccard similarity index [28], also known as the Tanimoto coefficient, is used to measure the similarity of two clusters. It is defined as the ratio of the number of common pixels between the ground truth and segmented image to the number of identical pixels of ground truth and segmented image:

$$J = \frac{I_{gt} \cap I_{seg}}{I_{gt} \cup I_{seg}} \quad (10)$$

where I_{gt} is the ground truth image and I_{seg} is the segmented image. The Jaccard index is zero if the two clusters are disjoint, i.e. they

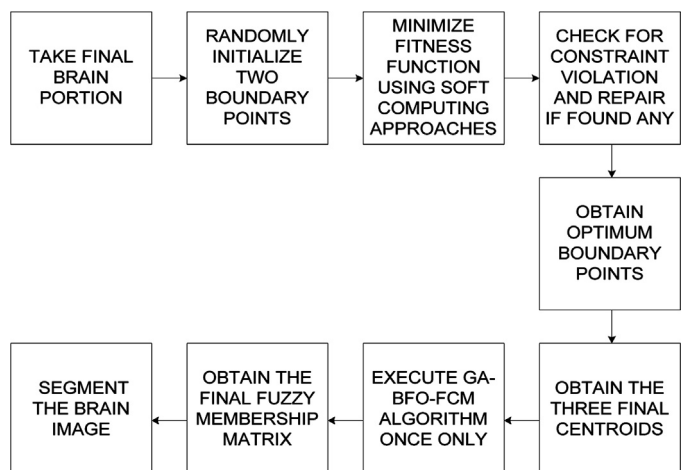


Fig. 4. Block diagram for the proposed MR brain image segmentation method.

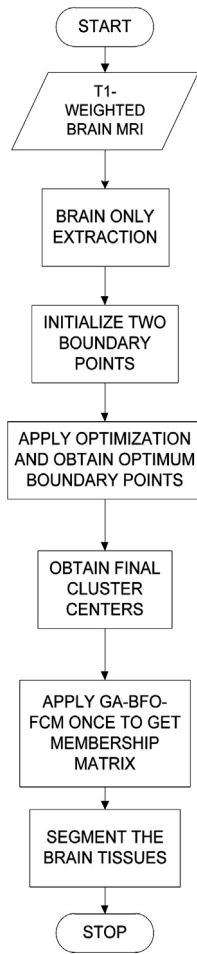


Fig. 5. Flow chart of the proposed method.

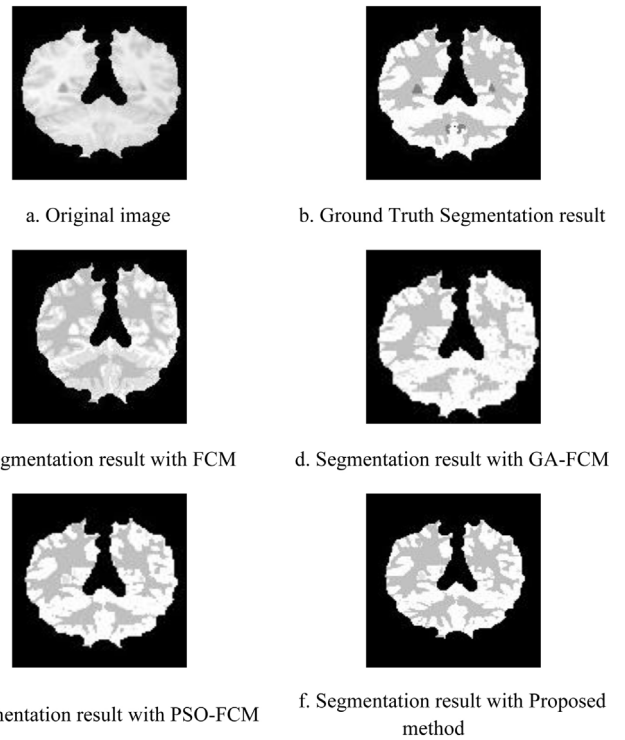


Fig. 6. Simulated T1 weighted slice 15 of MR Image 1.24.

The 15th slice of the brain only region of the simulated image and its segmented results using the proposed method is shown in Figs. 6–10. The regions only show GM, WM and CSF. The background pixels are removed during the brain extraction process. It may be noted that we deal with a simulated database with ground truth. Hence, noise filtering is not required before the brain extraction process. Here Table 2 shows the segmentation results with K-Means, FCM and soft computing techniques. The number of pixels in the three regions of the brain image is obtained from the

510 have no common pixels and one if they are identical. A higher value
511 of this index indicates better segmentation result.

512 The Dice coefficient [29] is another index like the Jaccard simi-
513 larity index for measuring the similarity of two clusters. It is defined
514 as [29]:

$$515 D = 2 \times \frac{I_{gt} \cap I_{seg}}{I_{gt} + I_{seg}} \quad (11)$$

516 A higher value of the Dice coefficient indicates more accurate seg-
517 mentation.

518 The false positive rate and the false negative rate are also used
519 to validate the clustering phenomenon. The false positive rate indi-
520 cates the possibility of pixels belonging to a cluster, but is not
521 segmented into that cluster. The false negative rate indicates the
522 possibility of pixels not belonging to a cluster, but is segmented
523 into that cluster. They are calculated as:

$$524 f_{pr} = \frac{N_{seg} - N(I_{gt} + I_{seg})}{N_{gt}} \quad (12)$$

525 and

$$526 f_{nr} = \frac{N_{gt} - N(I_{gt} + I_{seg})}{N_{gt}} \quad (13)$$

527 where f_{pr} is false positive rate, N_{seg} is the number of pixels in the
528 segmented image, $N(I_{gt} + I_{seg})$ is the number of pixels common to
529 ground truth and segmented image, N_{gt} is the number of pixels in
530 the ground truth image and f_{nr} is false negative rate. Lower values
531 of these rates indicate better segmentation result.

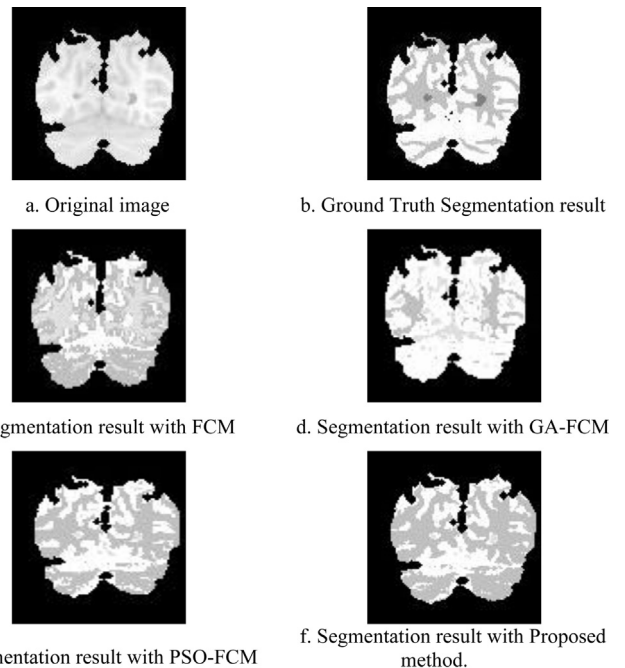


Fig. 7. Simulated T1 weighted slice 15 of MR Image 4.8.

Table 2
Segmentation result with FCM and soft computing techniques.

Serial no.	Images	Brain tissues	Number of pixels						
			Ground truth	K-means	FCM	GA-FCM	PSO-FCM	BFO-FCM	Proposed method
1	1.24	GM	3592	2694	2788	3991	3802	3313	3608
		WM	2916	2489	2489	2275	2613	3258	2890
		CSF	119	1444	1350	361	212	56	129
2	4.8	GM	3278	1429	2724	3821	2782	3011	3252
		WM	1988	1276	1335	1384	2464	2251	2006
		CSF	69	2630	1276	130	89	77	73
3	5.8	GM	4681	3740	3740	5064	4516	3952	4762
		WM	2829	2331	2331	2370	2938	3487	2729
		CSF	68	1507	1507	144	124	139	87
4	100.23	GM	8423	2796	6443	8162	7710	6738	8487
		WM	4065	3568	3787	3898	4627	5705	3936
		CSF	342	6466	2600	770	493	407	387
5	11.3	GM	8471	2292	6815	8554	3717	9951	9551
		WM	3997	3909	3909	2978	9130	3297	3304
		CSF	0	6671	2148	1340	25	24	17

Table 3
Segmentation evaluation with Jaccard similarity index.

Serial no.	Images	Brain tissues	K-means	FCM	GA-FCM	PSO-FCM	BFO-FCM	Proposed method
1	1.24	GM	0.4999	0.5209	0.7151	0.8025	0.8034	0.9636
		WM	0.7560	0.6776	0.7500	0.7819	0.7933	0.8102
		CSF	0.0547	0.0569	0.1330	0.2500	0.2560	0.3030
2	4.8	GM	0.3766	0.4874	0.5625	0.6191	0.6308	0.7167
		WM	0.5587	0.3604	0.5344	0.5587	0.5765	0.6254
		CSF	0.0026	0.0379	0.0628	0.3056	0.3293	0.3335
3	5.8	GM	0.5892	0.4325	0.5892	0.6095	0.7202	0.7837
		WM	0.7468	0.5160	0.6083	0.6453	0.7468	0.7561
		CSF	0.0153	0.0153	0.0357	0.1892	0.2090	0.2241
4	100.23	GM	0.2860	0.3864	0.6366	0.6625	0.7163	0.7753
		WM	0.8178	0.4423	0.579	0.6995	0.8359	0.9033
		CSF	0.0026	0.0061	0.0078	0.0128	0.0134	0.0194
5	11.3	GM	0.2129	0.3278	0.3747	0.7191	0.7823	0.8278
		WM	0.8263	0.4173	0.4359	0.7214	0.8263	0.4173
		CSF	0	0	0	0	0	0

ground truth image. It is observed that the result obtained with our proposed method is closer to the ground truth. The performance measures for K-Means, FCM, GA-FCM, PSO-FCM, BFO-FCM and our method are displayed in Tables 3–6. It is observed that soft computing approaches significantly improve the segmentation result as compared with FCM alone. Note that our method yield better results as compared to K-Means, FCM, GA-FCM, PSO-FCM and BFO-FCM. In this paper, we have considered five different cases. FCM alone does not give us satisfactory results. GA-FCM, PSO-FCM and BFO-FCM are the only contenders. But it is seen

that our method gives more accurate results than other mentioned methods. While considering Image 11_3, with CSF=0 in the ground truth image, GA-FCM gives a false idea about the number of pixels i.e. 1340. However, our method misclassifies only 17 pixels.

It is observed from Tables 3–6 that segmentation indices obtained by our method are better than K-Means, FCM, GA-FCM, PSO-FCM and BFO-FCM. It is also observed that for Image 11_3, value of CSF in the manual segmentation is zero. When this image is segmented using FCM, it gives highly misclassified clusters. The

Table 4
Segmentation evaluation with Dice coefficient.

Serial no.	Images	Brain tissues	K-means	FCM	GA-FCM	PSO-FCM	BFO-FCM	Proposed method
1	1.24	GM	0.6666	0.6850	0.8339	0.8910	0.8924	0.9813
		WM	0.8611	0.8611	0.8679	0.8776	0.8847	0.8956
		CSF	0.1037	0.1077	0.2348	0.4076	0.4080	0.4651
2	4.8	GM	0.5472	0.6553	0.7200	0.7648	0.7935	0.8350
		WM	0.7169	0.7169	0.7298	0.7314	0.7966	0.7995
		CSF	0.0052	0.0730	0.1182	0.4651	0.4954	0.4989
3	5.8	GM	0.7415	0.7415	0.8374	0.8574	0.9039	0.9787
		WM	0.8550	0.8550	0.8844	0.9565	0.9807	0.9880
		CSF	0.0300	0.0300	0.0689	0.3182	0.3457	0.3509
4	100.23	GM	0.4448	0.7970	0.8347	0.8779	0.9574	0.9773
		WM	0.8998	0.9106	0.9232	0.9334	0.9433	0.9825
		CSF	0.0052	0.0121	0.0154	0.0253	0.0265	0.0286
5	11.3	GM	0.3510	0.8366	0.8779	0.5451	0.4937	0.4938
		WM	0.9049	0.9049	0.8381	0.6071	0.5889	0.5889
		CSF	0	0	0	0	0	0

Table 5
Segmentation evaluation with false negative rate.

Serial no.	Images	Brain tissues	K-means	FCM	GA-FCM	PSO-FCM	BFO-FCM	Proposed method
1	1.24	GM	0.2223	0.3917	0.0966	0.0830	0.0589	0.0553
		WM	0.0651	0.4020	0.3086	0.1529	0.1142	0.1825
		CSF	0.9446	0.2121	0.1545	0.1457	0.1359	0.1349
2	4.8	GM	0.0987	0.4001	0.2205	0.2103	0.1379	0.1279
		WM	0.0831	0.4115	0.1378	0.1207	0.0820	0.0754
		CSF	0.9973	0.1774	0.1535	0.1377	0.1145	0.0973
3	5.8	GM	0.1652	0.3330	0.2284	0.2069	0.1653	0.0402
		WM	0.0536	0.2202	0.0085	0.0046	0.0025	0.0020
		CSF	0.9847	0.0417	0.0417	0.0416	0.0412	0.0405
4	100.23	GM	0.1077	0.2967	0.1782	0.1512	0.1043	0.0174
		WM	0.0376	0.1205	0.0950	0.0850	0.0520	0.0292
		CSF	0.9974	0.6364	0.6118	0.5318	0.4545	0.3897
5	11.3	GM	0.1758	0.2452	0.1178	0.6078	0.6571	0.1202
		WM	0.0849	0.1051	0.2687	0.0030	0.0020	0.0008
		CSF	NaN	NaN	NaN	NaN	NaN	NaN

Table 6
Segmentation evaluation with false positive rate.

Serial no.	Images	Brain tissues	K-means	FCM	GA-FCM	PSO-FCM	BFO-FCM	Proposed method
1	1.24	GM	0.5557	0.1679	0.1634	0.1414	0.1105	0.1125
		WM	0.2366	0.0556	0.0202	0.0133	0.0116	0.0144
		CSF	0.0132	1.8485	1.1010	0.6970	0.6566	0.2300
2	4.8	GM	1.3933	0.2309	0.1858	0.0817	0.0589	0.0169
		WM	0.6411	0.0533	0.0050	0.0049	0.0027	0.0015
		CSF	0.0209	20.7097	11.8387	10.7419	10.3226	10.3073
3	5.8	GM	0.4168	0.1320	0.1102	0.0060	0.0051	0.0047
		WM	0.2673	0.0442	0.0095	0.0063	0.0032	0.0023
		CSF	0.0006	61.8333	25.8750	25.0833	21.7917	21.0432
4	100.23	GM	2.1202	0.0616	0.0472	0.0392	0.0241	0.0237
		WM	0.1768	0.0522	0.0279	0.0255	0.0203	0.0054
		CSF	0.0042	58.7273	39.9091	34.3182	32.3864	10.3400
5	11.3	GM	2.8717	0.0497	0.0476	0.0466	0.0463	1.6840
		WM	0.1074	0.0831	0.0138	1.2872	1.3915	0.5823
		CSF	Inf	Inf	Inf	Inf	Inf	Inf

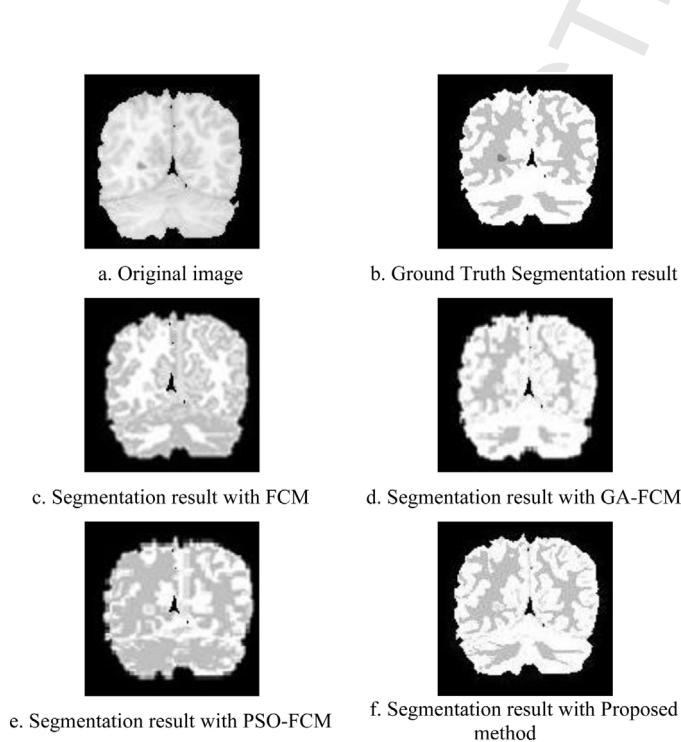


Fig. 8. Simulated T1 weighted slice 15 of MR Image 5.8.

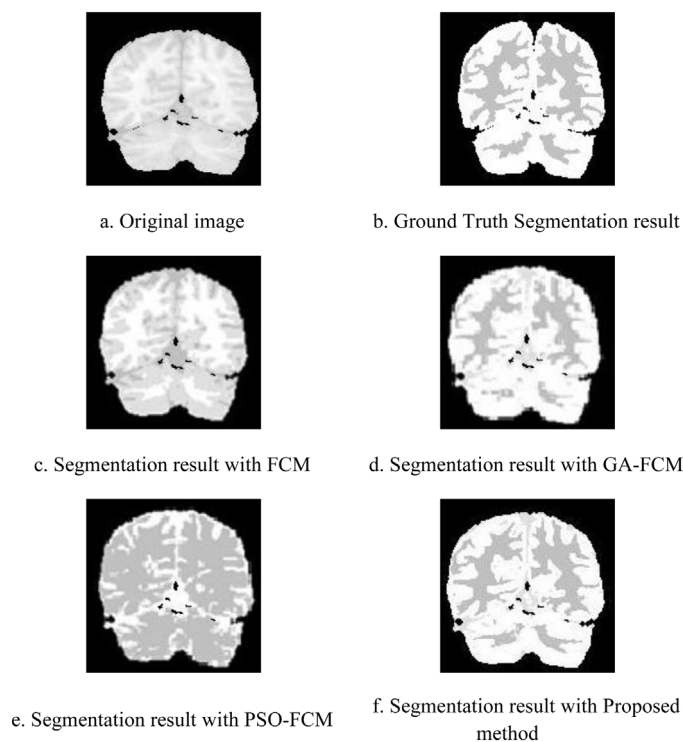


Fig. 9. Simulated T1 weighted slice 15 of MR Image 11.3.

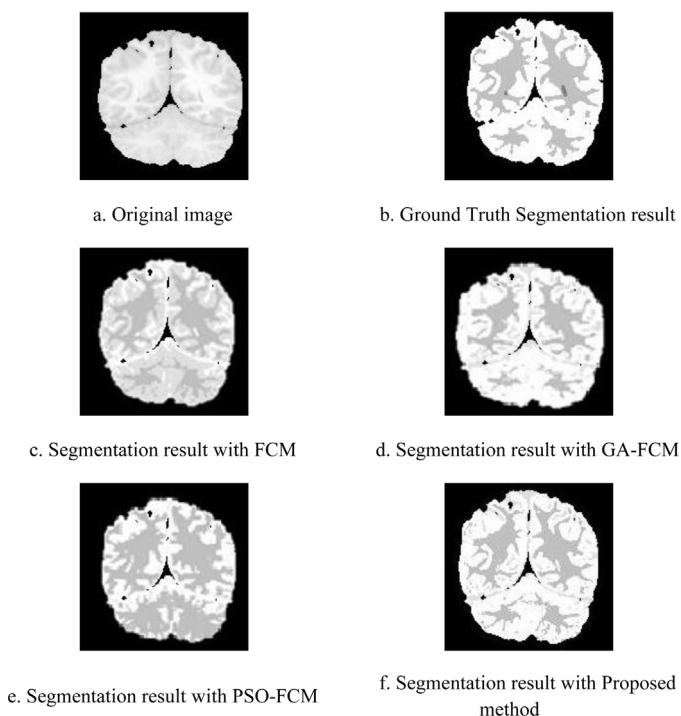


Fig. 10. Simulated T1 weighted slice 15 of MR Image 100.23.

Table 7
Percentage of pixels misclassified.

Serial no.	Images	Brain tissues	Percentage of pixels misclassified					
			K-means	FCM	GA-FCM	PSO-FCM	BFO-FCM	Proposed method
1	1.24	GM	25.00	22.38	11.11	5.85	7.77	0.45
		WM	14.64	14.64	21.98	10.39	11.73	0.89
		CSF	1113.45	1034.45	203.36	78.15	52.94	8.40
2	4.8	GM	56.41	16.90	16.56	15.13	8.15	0.79
		WM	35.81	32.85	30.38	23.94	13.23	0.91
		CSF	3711.59	1749.28	88.41	28.99	11.59	5.80
3	5.8	GM	20.10	20.10	8.18	3.52	15.57	1.73
		WM	17.60	17.60	16.22	3.85	23.26	3.53
		CSF	2116.18	2116.18	111.76	82.35	104.41	27.94
4	100.23	GM	66.81	23.51	3.10	8.46	20.00	0.76
		WM	12.23	6.84	4.11	13.83	40.34	3.17
		CSF	1790.64	660.23	125.15	44.15	19.01	13.16
5	11.3	GM	72.94	19.55	0.98	56.12	17.47	12.75
		WM	2.20	2.20	25.49	128.42	17.51	17.34
		CSF	Inf	Inf	Inf	Inf	Inf	Inf

Table 8
Performance measures for noisy brain images with the proposed method.

Serial no.	Noise level	Brain tissues	Jaccard index	Dice coefficient	False negative rate	False positive rate
1	0%	CSF	0.4951	0.6623	0.1220	0.5482
		GM	0.8086	0.8941	0.0358	0.1620
		WM	0.9387	0.9684	0.0504	0.0009
2	1%	CSF	0.4869	0.6549	0.1057	0.8368
		GM	0.8110	0.8957	0.0725	0.1466
		WM	0.9398	0.9690	0.0477	0.0160
3	3%	CSF	0.4918	0.6593	0.1817	0.6641
		GM	0.7555	0.8607	0.0532	0.2532
		WM	0.9056	0.9505	0.0887	0.0063
4	5%	CSF	0.4808	0.6493	0.1173	0.8360
		GM	0.7687	0.8693	0.0728	0.2062
		WM	0.9126	0.9543	0.0751	0.0134
5	7%	CSF	0.4660	0.6358	0.2580	0.5921
		GM	0.7563	0.8613	0.1445	0.1311
		WM	0.9007	0.9478	0.0149	0.0937
6	9%	CSF	0.4521	0.6227	0.2574	0.6423
		GM	0.7271	0.8420	0.1680	0.1443
		WM	0.8812	0.9369	0.0160	0.1167

reason being the fact that CSF is zero for Image 11_3. This is also evident from the segmentation indices that give unusual results. It may be reiterated the fact that our proposed evolutionary techniques are implemented for three clusters for segmentation.

The ground truth segmentation result is available from the datasets of IBSR. This helps us in defining the segmentation indices for comparing different segmentation techniques. It is observed from Figs. 6–10 that segmentation with our method is closest to the ground truth.

Fig. 11 shows the segmentation results with soft computing approaches. Fig. 11(a) shows the distribution of pixels for the original brain image data. It is observed that the pixels are distributed all over the region. Fig. 11(b)–(d) shows the segmentation result. From Fig. 11(b)–(d), it is seen that pixels are clearly divided into three clusters as per the regions of the brain. From Fig. 11(b), it is seen that there is an overlap between cluster 2 and 3. Moreover, cluster 1 is stretched, which is not desirable. As evident from Fig. 11(d), segmentation results obtained by using our method are more accurate than PSO-FCM and GA-FCM. The percentage of pixels misclassified is displayed in Table 7 to justify our claims. The percentages of misclassified pixels are computed as Eq. (14).

$$\%Mis = \frac{|N_{gt} - N_{seg}|}{N_{gt}} \times 100 \quad (14)$$

where N_{gt} is the number of pixels in the ground truth for a particular brain tissue and N_{seg} is the number of pixels in the segmented image of the same brain tissue. The lower is the percentage of misclassification better is the segmentation. It is to be noted that our

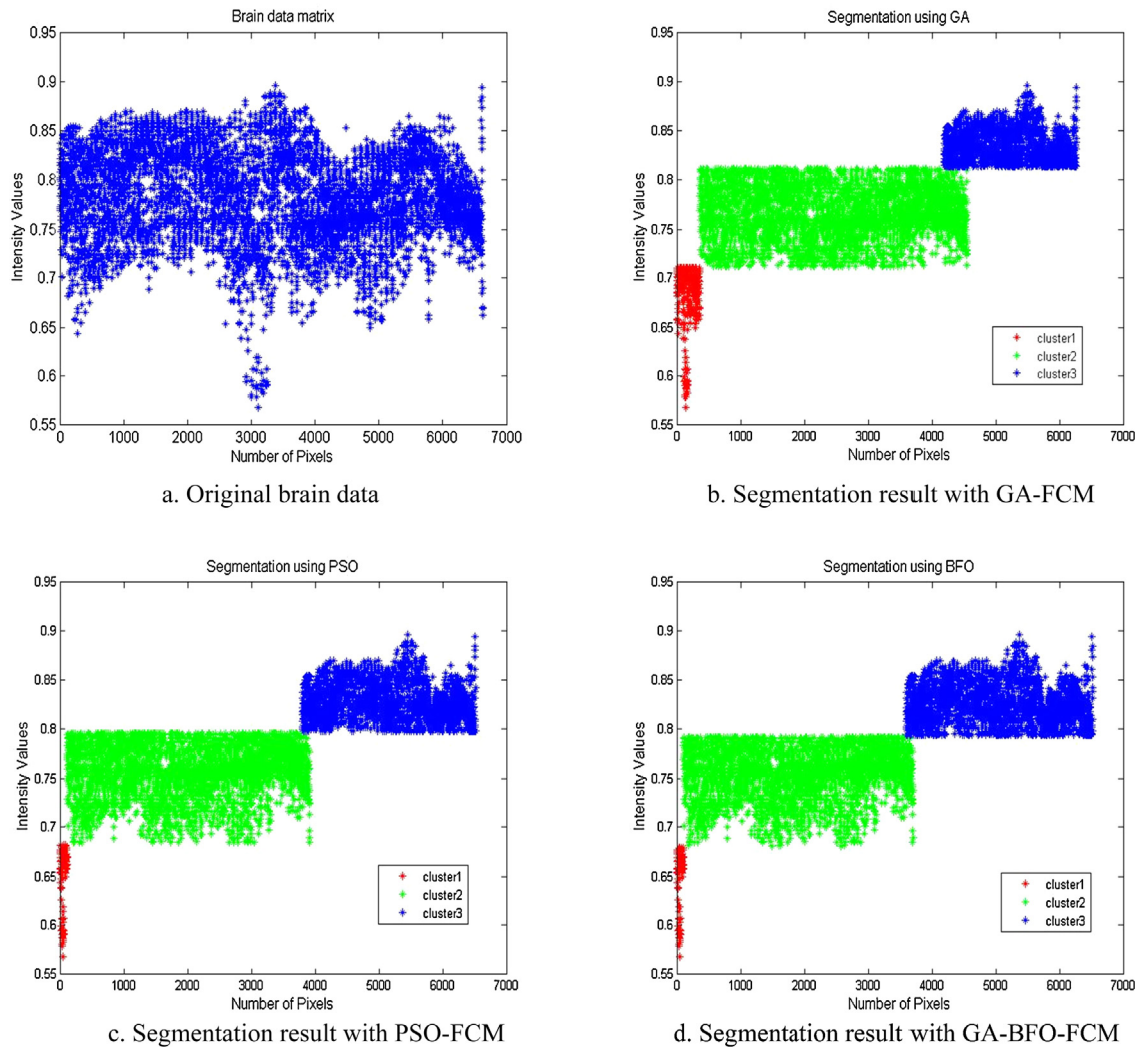


Fig. 11. Segmentation result of simulated T1 weighted slice 15 of MR Image 1.24.

586 proposed method gives the minimum misclassified pixel percent-
587 age as compared to other methods used in the paper.

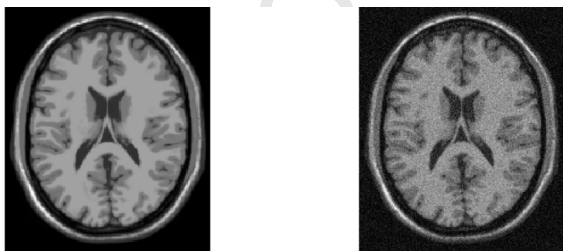
588 To validate the robustness of our proposed method we have used
589 MR brain images from the Brainweb database [31] with additional
590 noise levels: 1%, 3%, 5%, 7% and 9%. The main cause of this noise
591 is tissue motion or external RF interference. This noise assumes
592 salt and pepper form. The median filter being a non-derivative, low
593 pass type removes such noise efficiently. Thus, the brain image
594 is processed by a median filter before the brain extraction pro-
595 cess to remove the noise for improved clustering performance. The
596 segmentation performance parameters are calculated for different

597 noise levels and presented in Table 8. The details of the image used
598 are: modality = T1, protocol = ICBM, phantom-name = normal, slice-
599 thickness = 1 mm, INU = 0%. Note that Fig. 12(a) represents coronal
600 view of 90th slice of T1_icbm_normal.1mm.pn0.rf0, a simulated
601 normal brain phantom of $181 \times 217 \times 181$ voxels with 1 mm^3
602 for each voxel without any noise or intensity inhomogeneity.

603 It is observed that with addition of noise the performance
604 parameters change marginally, thus validating the robustness of
605 our proposed method.

606 **Conclusion**

607 The MR brain image is segmented using the proposed method. It
608 is observed that the use of soft computing techniques significantly
609 improves segmentation results as compared to results obtained
610 with FCM and similar methods implemented alone. Further, our
611 proposed OBPD method using GA-BFO yield better segmentation
612 results as compared to FCM, K-Means, GA-FCM, PSO-FCM, and
613 BFO-FCM techniques. The advantage of our method lies in its abil-
614 ity to compute the final cluster centroids using optimum boundary
615 point information. Other benefits are – improved segmentation
616 accuracy due to in-built constraint handling, the proposed GA-BFO
617 algorithm gets additional nutrition for searching optimum values
618 etc. It may be noted that the proposed evolutionary techniques
619 would give inaccurate segmentation results for images having



a. Brain image with 0% noise. b. Brain image with 9% noise.

Fig. 12. Noisy brain images from Brainweb database.

clusters different from the predefined values (here we have defined three clusters). From the results, it is observed that with addition of noise the performance parameters change slightly, thus confirming the robustness of our method.

The future work in this direction can include optimization of scalar weighting exponent m using evolutionary computation (EC) techniques. The proposed technique can be extended to find out number of boundary points required for clustering, when a ground truth image is not available. Our proposed technique can also be extended for noisy MR images (without ground truth) by using a suitable filter before brain extraction process.

Acknowledgment

The authors would like to thank the anonymous reviewers for their critical and constructive comments and suggestions for significant improvement of this paper.

References

- [1] M. Forouzanfar, N. Forghani, M. Teshnehlab, Parameter optimization of improved fuzzy c-means clustering algorithm for brain MR image segmentation, *Eng. Appl. Artif. Intell.* 23 (2) (2010) 160–168.
- [2] H. Suzuki, J. Toriwaki, Automatic segmentation of head MRI images by knowledge guided thresholding, *Comput. Med. Imaging Graph.* 15 (40) (1991) 233–240.
- [3] J.A. Canny, A computational approach to edge detection, *IEEE Trans. Pattern Anal. Mach. Intell.* 6 (1986) 679–698.
- [4] R. Pohle, K.D. Toennies, Segmentation of medical images using adaptive region growing, in: *Proceedings of SPIE Medical Imaging*, 2001, p. 4322.
- [5] W.M. Wells III, W.E.L. Grimson, R. Kikinis, F.A. Jolesz, Adaptive segmentation of MRI data, *IEEE Trans. Med. Imaging* 15 (4) (1996) 429–442.
- [6] C.L. Li, D.B. Goldgof, L.O. Hall, Knowledge-based classification and tissue labeling of MR images of human brain, *IEEE Trans. Med. Imaging* 12 (4) (1993) 740–750.
- [7] J.C. Dunn, A fuzzy relative of the ISODATA process and its use in detecting compact well-separated clusters, *J. Cybern.* 3 (1973) 32–57.
- [8] J.C. Bezdek, *Pattern Recognition With Fuzzy Objective Function Algorithms*, Kluwer Academic Publishers, New York, 1981.
- [9] S. Nie, Y. Zhang, W. Li, Z. Chen, A fast and automatic segmentation method of MR brain images based on genetic fuzzy clustering algorithm, in: *Proceedings of International Conference on Engineering in Medicine and Biology Society*, 2007, pp. 5628–5633.
- [10] L.O. Hall, J.C. Bezdek, S. Boggavarapu, A. Bensaid, Genetic fuzzy clustering, in: *Fuzzy Information Processing Society Biannual Conference. Industrial Fuzzy*

- Control and Intelligent Systems Conference and the NASA Joint Technology Workshop on Neural Networks and Fuzzy Logic, 1994, pp. 411–415.
- [11] L.O. Hall, I.B. Ozyurt, J.C. Bezdek, Clustering with a genetically optimized approach, *IEEE Trans. Evol. Comput.* 3 (2) (1999) 103–112.
- [12] L. Li, X. Liu, M. Xu, A novel fuzzy clustering based on particle swarm optimization, in: *First IEEE International Symposium on Information Technologies and Applications in Education*, 2007, pp. 88–90.
- [13] B.J. Zhao, An ant colony clustering algorithm, in: *Proceedings of Sixth International Conference on Machine Learning and Cybernetics*, 2007, pp. 3933–3938.
- [14] O. Castillo, E. Rubio, J. Soria, E. Naredo, Optimization of the fuzzy C-means algorithm using evolutionary methods, *Eng. Lett.* 20 (1) (2012).
- [15] E.R. Hruschka, R.J.G.B. Campello, A.A. Freitas, A.P.L.F. De Carvalho, A survey of evolutionary algorithms for clustering, *IEEE Trans. Syst. Man Cybern. – Part C: Appl. Rev.* 39 (2) (2009) 133–155.
- [16] A. Mukhopadhyay, U. Maulik, A multiobjective approach to MR brain image segmentation, *Appl. Soft Comput.* 11 (2011) 872–880.
- [17] K.O. Lim, A. Pfefferbaum, Segmentation of MR brain images into cerebrospinal fluid spaces, white and gray matter, *J. Comput. Assist. Tomogr.* 13 (4) (1989) 588–593.
- [18] J. Yu, Q. Cheng, H. Huang, Analysis of the weighting exponent in the FCM, *IEEE Trans. Syst. Man Cybern., Part B: Cybern.* 34 (1) (2004) 634–639.
- [19] S. Shen, W. Sandham, M. Granat, A. Sterr, MRI fuzzy segmentation of brain tissue using neighborhood attraction with neural-network optimization, *IEEE Trans. Inf. Technol. Biomed.* 9 (2005) 459–467.
- [20] R.J. Hathaway, J.C. Bezdek, Optimization of clustering criteria by reformulation, *IEEE Trans. Fuzzy Syst.* 3 (2) (1995) 241–245.
- [21] D.E. Goldberg, *Genetic Algorithms in Search, Optimization and Machine Learning*, Addison Wesley, 1989
- [22] J. Kennedy, R.C. Eberhart, Particle swarm optimization, in: *Proceedings of the IEEE International Conference on Neural Networks*, 1995, pp. 1942–1948.
- [23] K.M. Passino, Biomimicry of bacterial foraging for distributed optimization and control, *IEEE Control Syst.* 22 (3) (2002) 52–67.
- [24] S. Das, A. Biswas, S. Dasgupta, A. Abraham, Bacterial foraging optimization algorithm: theoretical foundations, analysis and applications *Found. Comput. Intell.*, 3, Springer, Berlin, Heidelberg, 2009, pp. 23–55.
- [25] MR Brain image database: <http://www.cma.mgh.harvard.edu/ibsr/>
- [26] K. Somasundaram, T. Kalaiselvi, Automatic brain extraction methods for T1 magnetic resonance images using region labeling and morphological operations, *Comput. Biol. Med.* 41 (8) (2011) 716–725.
- [27] P.N. Tan, *Introduction to Data Mining*, Pearson Education India, 2007.
- [28] P. Jaccard, The distribution of the flora in the alpine zone, *New Phytol.* 11 (2) (1912) 37–50.
- [29] L.R. Dice, Measures of the amount of ecologic association between species, *Ecology* 26 (3) (1945) 297–302.
- [30] R. Cárdenes, R. de Luis-García, M. Bach-Cuadra, A multidimensional segmentation evaluation for medical image data, *Comput. Methods Programs Biomed.* 96 (2) (2009) 108–124.
- [31] Brainweb: Simulated Brain Database, Available at: <http://www.bic.mni.mcgill.ca/brainweb/>

Q5